Lattice modulation spectroscopy of strongly interacting bosons in disordered and quasiperiodic optical lattices

G. Orso,[1] A. Iucci,[2,3] M. A. Cazalilla,[4,5] and T. Giamarchi[3]

[1]*Laboratoire Physique Théorique et Modèles Statistiques, Université Paris Sud, Bat. 100, 91405 Orsay Cedex, France*

[2]*Instituto de Física la Plata (IFLP)–CONICET and Departamento de Física, Universidad Nacional de La Plata, CC 67, 1900 La Plata, Argentina*

[3]*DPMC-MaNEP, University of Geneva, 24 Quai Ernest Ansermet, CH-1211 Geneva 4, Switzerland*

[4]*Centro de Física de Materiales (CSIC-UPV/EHU), Edificio Korta, Avenida de Tolosa 72, 20018 San Sebastián, Spain*

[5]*Donostia International Physics Center (DIPC), Manuel de Lardizábal 4, 20018 San Sebastián, Spain*

We compute the absorption spectrum of strongly repulsive one-dimensional bosons in a disordered or quasiperiodic optical lattice. At commensurate filling, the particle-hole resonances of the Mott insulator are broadened as the disorder strength is increased. In the noncommensurate case, mapping the problem to the Anderson model allows us to study the Bose-glass phase. Surprisingly, we find that a perturbative treatment in both cases, weak and strong disorders, gives a good description at all frequencies. In particular, we find that the infrared-absorption rate in the thermodynamic limit is quadratic in frequency. This result is unexpected since for other quantities, like the conductivity in one-dimensional systems, perturbation theory is only applicable at high frequencies. We discuss applications to recent experiments on optical lattice systems and, in particular, the effect of the harmonic trap.

PACS number(s): 03.75.Lm, 71.23.−k, 61.44.Fw

I. INTRODUCTION

In recent years, developments in the field of ultracold atomic gases have considerably enlarged the possibilities for exploring the physics of strongly correlated systems [1]. For instance, the study of quantum phase transitions, a subject of continuous theoretical interest, has been strongly stimulated by the experimental observation of the superfluid to Mott insulator transition using optical lattices [2]. Indeed, ultracold atom systems offer us an unprecedented control over the system parameters, which can allow us to ultimately understand the physics of very hard problems such as the phase diagram of the Hubbard model in two dimensions [3].

A particularly interesting and fertile arena is the study of disordered ultracold atoms. Random potentials can be introduced in a controlled way by laser beams generating speckle patterns [4–9] or by loading in an optical lattice a mixture of two kinds of atoms, one heavy and one light. When the heavy atoms become randomly localized in the lattice, they will act as impurities for the lighter atoms [10]. Another available technique is to superimpose two optical lattices with incommensurate periodicities, thus, generating a quasiperiodic potential [11]. The quasiperiodic lattices as well as the speckle patterns have been recently used in the experimental efforts to observe the effects of Anderson localization in dilute Bose gases expanding in highly elongated traps [12,13]. Since Anderson localization is a single-particle effect, the next logical step is to study the interplay of disorder and interactions in strongly interacting ultracold atomic systems [14–17]. The latter may be accessible by tuning interparticle interactions using Feshbach resonances [18] or by loading the atoms in sufficiently deep optical lattices [9] and/or strongly confining them to low dimensions in tight traps [1].

In the context of the efforts described above, one of the experimental challenges is to observe in ultracold gases clear signatures of the theoretically predicted transition from a superfluid to the Bose-glass phase [19–21]. A pioneering step in this direction was recently taken by the Florence group by using lattice modulation spectroscopy [11]. This technique consists in heating an ultracold gas loaded in an optical lattice by periodically modulating the depth of the lattice [22–24]. When perturbed in this way, the gas is driven out of equilibrium and absorbs energy. When the perturbation is switched off, and after rethermalization, the broadening of the momentum distribution around zero momentum is taken as a measure of the energy absorbed by the system during the lattice modulation [22]. On the theory side, for nondisordered lattices, the calculation of the energy absorption rate due to the lattice modulation was first performed analytically within linear-response theory by some of the present authors [23]. These results were confirmed and extended beyond linear response using time-dependent density-matrix renormalization-group methods, both for the case of bosons [24] and fermions [25]. More recently, for disordered optical lattices, the energy absorption rate has been numerically calculated using full diagonalization in small systems [26,27]. Other methods that have also been discussed in the literature for detecting signatures of the effect of disorder (or quasiperiodicity) on interacting boson systems in one dimension focus on the momentum distribution [16,28], the expansion dynamics in quasiperiodic potentials [15], and the dipole oscillations in the presence of defects [29].

Let us consider a one-dimensional disordered Bose gas described by the following Hamiltonian:

$$H = -J \sum_j (b_{j+1}^\dagger b_j + \text{H.c.}) + \frac{U}{2} \sum_j n_j(n_j - 1) + \sum_j (\epsilon_j + V_j^{\text{ho}}) n_j,$$

(1)

where b_j denotes the boson annihilation operator at sites j, $n_j = b_j^\dagger b_j$ being the local density. Here J and U are the usual

parameters of the Bose-Hubbard model corresponding to the tunneling rate and the on-site repulsion ($U > 0$). The last term in the right-hand side of Eq. (1) accounts for the presence of both the harmonic trap V_j^{ho} and the disorder potential ϵ_j.

The distribution of the on-site energies ϵ_j in Eq. (1) depends on the specific choice of the random (or pseudorandom) potential. In this work, we extensively compare two cases

$$(a)\, \epsilon_j \text{ uniformly distributed in} [-\Delta, \Delta], \qquad (2)$$

$$(b)\, \epsilon_j = \Delta \cos(2\pi j\sigma), \quad \sigma \text{ irrational}, \qquad (3)$$

where Δ measures the strength of the disorder. From the experimental point of view, speckle patterns and lattice containing heavy atom impurities can be modeled by case (a), whereas quasiperiodic potentials obtained by superimposing two optical potentials with incommensurate periodicities $d_1/d_2 = \sigma$ are described by case (b).

In this work, we assume that the hopping amplitude J in Eq. (1) is modulated periodically in time according to $J(t) = J + \delta J \cos \omega t$, where ω is the modulation frequency. We calculate the energy absorption rate within linear-response theory, which is valid for weak lattice modulations $\delta J \ll J$.

We shall restrict ourselves to the strongly repulsive regime of Eq. (1), where the on-site repulsion is large compared to both the hopping amplitude and the disorder strength ($U \gg J, \Delta$). We first discuss systems in the thermodynamic limit by setting $V_j^{\text{ho}} = 0$. Effects of the harmonic trapping potential will be discussed later, in Sec. V. We also set $\hbar = 1$ to simplify the notation.

In the thermodynamic limit, both the number N of bosons and the length M of the chain diverge. The ratio $\nu = N/M$ is instead finite and corresponds to the *filling* factor, i.e., the average number of bosons per lattice site. We must distinguish between two physically different situations. For *incommensurate fillings* $\nu < 1$, the system has gapless excitations. Thus, a good approximation to the absorption rate at frequencies $\omega \ll U$ can be obtained by formally taking $U \to +\infty$ and mapping the resulting hard-core bosons to noninteracting fermions using a Jordan-Wigner transformation (see, e.g., Ref. [30]). The resulting single-particle problem can be easily solved for a given choice of ϵ_i and V^{ho} and the energy absorption obtained. On the other hand, for *unit filling* ($\nu = 1$), the ground state is a Mott insulator with a gap. In this case, the elementary excitations are particles and holes [23] and, in a homogeneous system, the absorption can only occur at frequencies $\omega \sim U$. In the absence of disorder, the response of the system to the lattice modulation has been computed using degenerate perturbation theory within the subspace of particle and hole excitations [23]. The same methods can be generalized to deal with disordered case, as shown below.

The resulting general picture of the energy absorption is depicted in Fig. 1. The low frequency $0 < \omega < W$, where $W \sim \max(4J, 2\Delta)$ is the effective bandwidth, is only present for incommensurate fillings, $\nu < 1$. A second distribution is centered at frequency $\omega = U$ and comes from particle-hole excitations generating doubly occupied sites. The width of this absorption line is also given by W.
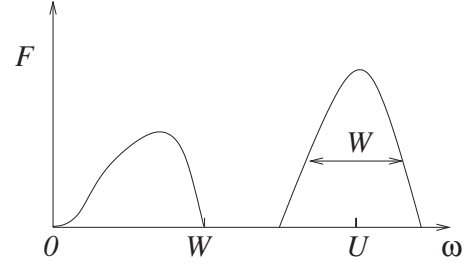

FIG. 1. Sketch of the full absorption spectrum at incommensurate filling. Here, $W \sim \max(4J, 2\Delta)$ is the effective bandwidth. The peak at $\omega \sim U$ stems from particle-hole excitations, whereas the low-frequency absorption appears as a consequence of the formation of a Bose glass at incommensurate filling.

The paper is organized as follows. In Sec. II, we present the general formalism needed to calculate the absorption rate for incommensurate and unit filling. In Secs. III and IV, we present our analytical and numerical results obtained for the random and the quasiperiodic potential, respectively. In Sec. V, we discuss the effects of a trapping potential. Finally in Sec. VI, we provide our conclusions. A derivation of the general formula [see Eq. (9)] for the absorption rate valid for weak disorder is given in the Appendix).

II. ENERGY ABSORPTION: LINEAR-RESPONSE THEORY

For weak perturbations, corresponding to $\delta J \ll J$, the energy absorption rate $\dot{E}_\omega$ can be calculated using the linear-response theory. The general formula has been first derived in Ref. [23] and in the presence of disorder it takes the form

$$\dot{E}_\omega = \frac{1}{2} \delta J_0^2 \omega \, \overline{\text{Im}[-\chi_K(\omega)]}, \qquad (4)$$

where $\chi_K(\omega)$ is the Fourier transform of the *retarded* correlation function $\chi_K(t) = -i\Theta(t)\langle [K(t), K(0)] \rangle$ of the hopping operator $K = -\Sigma_j (b_{j+1}^\dagger b_j + \text{H.c.})$, being $\Theta(t)$ the step function. In Eq. (4), the bar means average over different disorder (Sec. IV) or quasiperiodic (Sec. III) realizations.

In general, the calculation of the correlation function in Eq. (4) is a complicated many-body problem. However, in the limit of strong repulsion where $U \gg J, \Delta$, calculations are considerably simplified by the fact that we can accurately restrict ourselves to work within a subspace of the total Hilbert space, whose detailed structure depends on the filling. In the case of an *incommensurate* filling (i.e., $\nu < 1$), this subspace can be described in terms of noninteracting fermion states (that is, Slater determinants). For commensurate filling (i.e., *unit filling*, $\nu = 1$), we can restrict ourselves to the subspace with one particle and one hole excitation, as described below.

A. Incommensurate filling

For filling $\nu < 1$ and large on-site repulsion $J, \Delta \ll U$, we take the hard-core limit $U \to +\infty$. Bosons are then mapped onto *noninteracting* spinless fermions via the Jordan-Wigner transformation,

$$c_j = \exp\left[i\pi\sum_{k=1}^{j-1} n_k\right] b_j, \qquad (5)$$

where c_j satisfy fermionic commutation relations $\{c_j, c_j\} = 0$ and $\{c_j, c_j^\dagger\} = 1$. Under the above transformation, the Hamiltonian (1) is mapped onto the single-particle Hamiltonian

$$H' = -J\sum_j (c_{j+1}^\dagger c_j + \text{H.c.}) + \sum_j \epsilon_j c_j^\dagger c_j, \qquad (6)$$

where the on-site repulsion U has disappeared and the hopping operator K in Eq. (4) is now given by $K' = -\Sigma_j(c_{j+1}^\dagger c_j + \text{H.c.})$. Notice that the mapping of observables that are nonlocal in space is far less trivial, an example is the momentum distribution studied in Ref. [28] for disordered hard-core bosons in one dimension.

After some algebra, the absorbtion rate (4) becomes

$$\dot{E}_\omega = \frac{\delta J_0^2 \pi \omega}{2} \sum_{\alpha,\beta} \overline{\mathcal{K}_{\alpha\beta}[f(\varepsilon_\alpha) - f(\varepsilon_\beta)]\delta(\omega + \varepsilon_\alpha - \varepsilon_\beta)}, \quad (7)$$

where the matrix $\mathcal{K}$ is defined as

$$\mathcal{K}_{\alpha\beta} = \left|\sum_j [\psi_\alpha^*(j+1)\psi_\beta(j) + \psi_\alpha^*(j)\psi_\beta(j+1)]\right|^2. \qquad (8)$$

In the previous expressions ε_α and $\psi_\alpha(j)$ are the eigenvalues and eigenfunctions of H', respectively. In Eq. (7), $f(\varepsilon) = \{\exp[(\varepsilon - \mu)/T] + 1\}^{-1}$ is the Fermi-Dirac distribution function at a temperature T and chemical potential μ. The latter is fixed by the normalization condition $\nu = \Sigma_\alpha f(\varepsilon_\alpha)$. At zero temperature, the only relevant processes in Eq. (7) correspond to transitions from an occupied level [with energy $\varepsilon_\alpha < \mu(T=0)$] to an unoccupied level [$\varepsilon_\beta > \mu(T=0)$]. In particular, for unit filling the absorption (7) vanishes, consistently, with the fact that a Mott insulator can only absorb at much higher frequencies $\omega \sim U$.

In the absence of disorder [i.e., for $\epsilon_i = 0$ in Eq. (6)], the hopping modulation commutes with the Hamiltonian H' and, therefore, the absorption rate vanishes to all orders, even beyond linear response. In the above expression, this is reflected in that, for $\epsilon_i = 0$, the eigenstates of H' become plane waves, $\psi_k(j) \propto e^{ikj}$, with energy dispersion $\epsilon_k = -2J\cos k$ (k being the lattice momentum). Thus, the matrix (8) is diagonal, i.e., $\mathcal{K}_{kk'} = 4\delta_{k,k'}\cos^2 k$, which, together with the factor $f(\varepsilon_k) - f(\varepsilon_{k'})$ in Eq. (7) makes $\dot{E}_\omega$ vanish.

At weak disorder (i.e., $J \gg \Delta$), the absorption rate (7) can be evaluated using the perturbation theory (the details can be found in the Appendix), which yields

$$\dot{E}_\omega = \frac{\delta J_0^2 \pi \omega}{2M} \sum_{k,k'} \frac{\overline{|V_{k-k'}|^2}}{J^2}[f(\varepsilon_k) - f(\varepsilon_{k'})]\delta(\omega + \varepsilon_k - \varepsilon_{k'}), \quad (9)$$

where $V_k = \frac{1}{\sqrt{M}}\Sigma_{j=0}^{M-1} e^{ikj}\epsilon_j$ is the Fourier transform of the disorder potential. Equation (9) shows that the perturbation expansion in disorder is well defined provided the Fourier transform V_k is finite.

Let us finally consider the so-called atomic limit, which corresponds to $J \ll \Delta$ (yet $\Delta \ll U$). In this limit, tunneling can be neglected and the eigenstates are given by $\psi_m(j) = \delta_{jm}$.

From Eq. (8), we find $\mathcal{K}_{jj'} = 1$ if j and j' are nearest neighbor and zero otherwise. The absorption rate (7) thus reduces to

$$\dot{E}_\omega = \frac{\delta J_0^2 \pi \omega}{2} \sum_{r=\pm 1}\sum_{j=0}^{L-1} \overline{[f(\varepsilon_j) - f(\varepsilon_{j+r})]\delta(\omega + \varepsilon_j - \varepsilon_{j+r})}. \qquad (10)$$

In Sec. III, we shall explicitly compare the results obtained using exact numerical diagonalization with the above results obtained both in the limit of weak (9) and strong (10) disorders. Finally, it is important to emphasize that Eq. (7) does not account for particle-hole excitations, which are relevant at much higher frequencies $\omega \sim U$. These excitations become particularly important at unit filling ($\nu = 1$), when the strongly repulsive Bose gas becomes a Mott insulator and the absorption at low frequency $\omega \ll U$ predicted by Eq. (7) vanishes because there are no empty sites (i.e., holes) in the ground state. The contribution to the absorption from particle-hole excitations at unit filling will be discussed next.

B. Unit filling

We next turn our attention to the *commensurate* case with $\nu = 1$. In the strong-coupling regime $U \gg J, \Delta$, the system is deep in the Mott insulator phase, corresponding to exactly one particle per site. In Ref. [23], it was shown that for clean systems the absorption rate is zero at low frequencies and exhibits a narrow peak of width $\sim J$ centered about $\omega = U$. In this section, we consider the broadening of such peak due to a disorder or quasiperiodic potential ϵ_i.

In order to obtain the energy absorption rate within linear response, we first use the spectral decomposition of the correlation function $\chi_K(\omega)$ in terms of the exact eigenstates of the unperturbed Hamiltonian. This yields the following expression for the energy absorption:

$$\dot{E}_\omega = \delta J_0^2 \omega \frac{\pi}{2} \sum_n \overline{|\langle\Psi_n|K|\Psi_0\rangle|^2 \delta(\omega + E_0 - E_n)}, \qquad (11)$$

where $|\Psi_n\rangle$ are the eigenstates of the original Hamiltonian (1) with energies E_n, and $|\Psi_0\rangle = |1, 1, \ldots, 1\rangle$ is the ground state in the Fock representation corresponding to one boson per lattice site. The low-energy states are particle-hole excitations $|\phi(m,j)\rangle = \frac{1}{\sqrt{2}}b_m^\dagger b_{m+j}|\Psi_0\rangle$ corresponding to double occupation at site m and an empty site $m+j$. These excitations are all degenerate with energy U in the absence of tunneling and (i.e., for $\Delta = J = 0$).

For finite values of Δ and J, the eigenstates Ψ_n can be calculated using degenerate perturbation theory by writing $|\Psi_n\rangle = \Sigma_{m,j} f_{m,j}|\phi(m,j)\rangle$, where the coefficients satisfy

$$\sum_{m',j'} \langle\phi(m,j)|H|\phi(m',j')\rangle f_{m',j'} = E f_{m,j}. \qquad (12)$$

The above matrix element and the energy absorption can be computed by taking into account that $\langle\phi(m,j)|K|\Psi_0\rangle = -\sqrt{2}\delta_{j,\pm 1}$, within the subspace containing just one particle and one hole. Hence, the matrix elements in Eq. (11) correspond to $\langle\Psi_n|K|\Psi_0\rangle = -\Sigma_{m,r=\pm 1}\sqrt{2}f_{m,r}$. Notice that a similar technique has been recently employed in Ref. [31] to calcu-
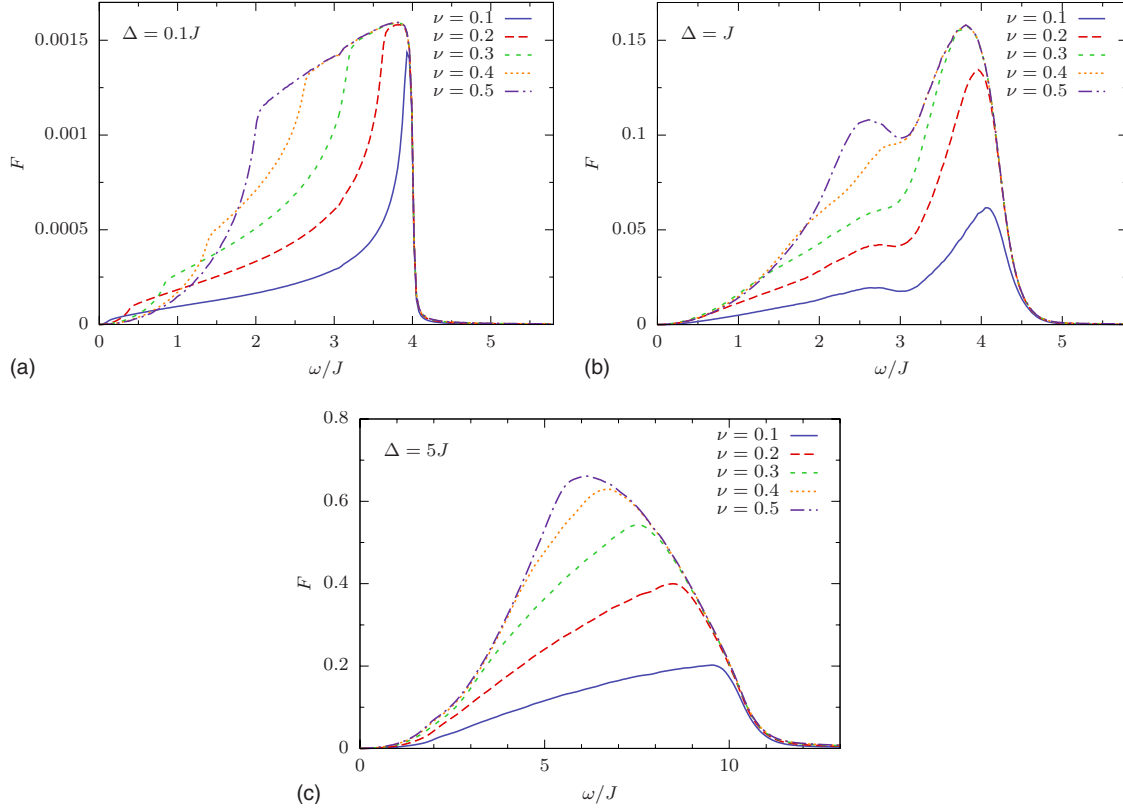
FIG. 2. (Color online) Energy absorption rate of hard-core bosons in a *random* potential: the response function F [see Eq. (14)] is plotted versus modulation frequency for different filling factors and increasing values of disorder strength: $\Delta = 0.1J$ (top panel), $\Delta = J$, and $\Delta = 5J$. Calculations are done on a ring of $M = 500$ lattice sites yielding negligible finite-size effects. The number of disorder realizations used was $N_r = 500$.

late the dynamic structure factor of a one-dimensional Mott insulator in a parabolic trap.

In the "atomic limit" where the tunneling can be neglected, Eq. (11) simplifies considerably. Localized particle-hole excitations become the exact eigenstates $|\Psi_n\rangle = |\phi(m, j)\rangle$ with energy $E_0 + U + \varepsilon_m - \varepsilon_{m+j}$, where $E_0 = \Sigma_{i=1}^M \varepsilon_i$ is the energy of the ground state for a given realization of ϵ_i. The absorption rate (11) then takes the form

$$\dot{E}_\omega = \delta J_0^2 \pi \omega \sum_{r=\pm 1} \sum_{m=1}^M \overline{\delta(\omega - U + \varepsilon_m - \varepsilon_{m+r})}, \quad (13)$$

which can be readily evaluated numerically once the disorder potential is known. We emphasize that Eq. (13) assumes that the system is a Mott insulator with exactly one atom per site. This condition is easily satisfied in the strong-coupling regime $J, \Delta \ll U$, where the disorder only broadens the absorption spectrum without affecting the nature of the ground state. A finite response at low frequency only occurs for stronger $\Delta \sim U$, where the system is close to the Bose-glass transition. In this limit, however, the random (or quasiperiodic) potential changes the occupation numbers at different sites, creating holes and doublons, so the ground state is no longer given by the Fock state $|\Psi_0\rangle$ and Eq. (13) ceases to be valid.

III. RESULTS FOR A DISORDER POTENTIAL

In this section, we assume that the on-site energy ϵ_i in Eq. (1) are random numbers uniformly distributed within the interval $[-\Delta, \Delta]$. The absorption rate (4) can thus be conveniently recast as

$$\dot{E}_\omega = M \delta J_0^2 F, \quad (14)$$

where F is a dimensionless function that can be numerically evaluated. The results for incommensurate and commensurate cases are described below.

A. Incommensurate filling

As stated above, the absorption rate is calculated numerically at zero temperature starting from Eqs. (7) and (8). In Fig. 2, we plot the frequency dependence of the response function F for *different* fillings and increasing values of disorder $\Delta = 0.1J$ (upper panel), $\Delta = J$ (central panel), and $\Delta = 5J$ (lower panel). Since, in the fermionic representation, the Hamiltonian of Eq. (6) is particle-hole symmetric, the absorption rate in Eq. (7) is unchanged under the transformation $\nu \rightarrow 1 - \nu$, so we restrict our discussion to fillings $\nu \leq 1/2$.

A noticeable feature of Fig. 2 is that the response at high frequencies is *independent* of the filling factor. In this limit, the relevant processes contributing to the absorption mainly

involve transitions from states far below the Fermi level [i.e., $(\varepsilon_\alpha \ll \mu)$] into empty states far above it [i.e., $(\epsilon_\beta \gg \mu)$]. As a result, the Fermi-Dirac distributions in Eq. (7) become irrelevant, and thus any dependence on the value chemical potential μ disappears.

However, at low frequencies, the absorption rate vanishes *quadratically* with frequency for any strength Δ of the disorder. To understand this, let us expand in Eq. (7) the distribution functions $f(\varepsilon_\alpha) - f(\varepsilon_\beta) \simeq (\varepsilon_\alpha - \varepsilon_\beta)\partial_\varepsilon f(\varepsilon_\alpha)$. Taking into account that, at zero temperature, $\partial_\varepsilon f(\varepsilon) = -\delta(\mu - \varepsilon)$, we find that $F \simeq C\omega^2$, where the constant

$$C = \frac{\pi}{2}\sum_{\alpha \neq \beta} \overline{\mathcal{K}_{\alpha\beta}\delta(\mu - \varepsilon_\alpha)\delta(\mu - \varepsilon_\beta)} \tag{15}$$

can be evaluated numerically. From Eq. (15), it can be seen that the constant C is nonzero provided there are nonvanishing matrix elements $\mathcal{K}_{\alpha\beta}$ connecting two states α and β at the Fermi level $\varepsilon_\alpha = \varepsilon_\beta = \mu$.

In the limit of weak disorder corresponding to $\Delta \ll J$, the absorption can be evaluated using Eq. (9), where $\overline{|V_k|^2} = \Delta^2/3M$, as follows from the expression for the Fourier transform of the disorder potential V_k. Going to the thermodynamic limit and introducing the density of states $\rho(\varepsilon) = (2\pi J\sqrt{1 - \varepsilon^2/4J^2})^{-1}$, we find

$$F = \frac{\omega\Delta^2}{24\pi J^4}\int_a^b \frac{d\epsilon}{\sqrt{1 - \epsilon^2/4J^2}\sqrt{1 - (\epsilon + \omega)^2/4J^2}}, \tag{16}$$

where $a = \max(-2J, \mu - \omega)$ and $b = \min(\mu, 2J - \omega)$. Here the chemical potential μ is related to the filling factor by $\mu = -2J\cos\pi\nu$. By expanding Eq. (16) at low frequencies, we again obtain that the quadratic behavior discussed above

$$F = \frac{\Delta^2\pi}{6J^2}\rho(\mu)^2\omega^2 = \frac{\Delta^2}{24\pi J^4}\frac{\omega^2}{\sin^2(\pi\nu)}. \tag{17}$$

It should be noticed that the right-hand side of Eq. (17) diverges in the limit of vanishing lattice filling $\nu \to 0$ because the density of states $\rho(\varepsilon)$ has a Van Hove singularity at zero energy in one dimension. Thus, the low filling limit, the quadratic behavior of Eq. (17) is only recovered at increasingly low frequencies, as shown in Fig. 2 (upper panel).

In Fig. 3, we show a comparison, in the limit of weak disorder ($\Delta = 0.01J$), of the numerical results (open symbols) obtained using exact diagonalization with the analytical expression of Eq. (16) (continuous lines). The agreement is indeed very good over the entire frequency range. In the inset, it is demonstrated that numerical results are consistent with the quadratic behavior of Eq. (17), expected at low frequencies.

On the other hand, in the opposite limit of strong disorder $\Delta \gg J$, the tunneling can be neglected. In this limit, the absorption rate can be evaluated directly from Eq. (10). Taking into account that the on-site energies ϵ_j at different sites are completely uncorrelated, we find

$$F = \pi\omega\int_{-\Delta}^{\bar\mu} d\epsilon\,\bar\rho(\epsilon)\int_{\bar\mu}^{\Delta} d\epsilon'\,\bar\rho(\epsilon')\delta(\omega + \epsilon - \epsilon'), \tag{18}$$

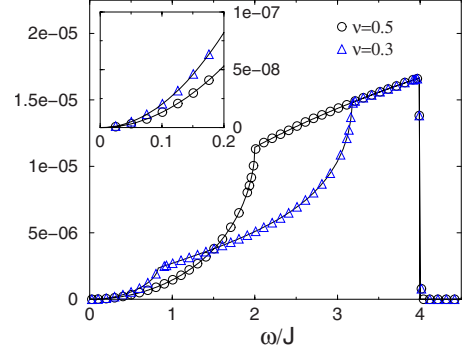where $\bar\mu$ and $\bar\rho$ are the *disorder-averaged* chemical potential

FIG. 3. (Color online) Comparison between numerics (symbols) and analytics [Eq. (9), solid line] for weak disorder. Here, $\Delta/J = 0.01$ and we consider two filling factors $\nu = 0.3$ and $\nu = 0.5$. The length of the chain is $M = 2000$ and the number of disorder realizations is $N_r = 2000$. The inset is a zoom of the low-frequency regime, where the absorption rate is quadratic in frequency as given by Eq. (17).

and density of states, respectively. In the random potential, the latter is constant and given by $\bar\rho(\epsilon) = 1/2\Delta$, and therefore $\bar\mu = (2\nu - 1)\Delta$. Using Eq. (18), the following low-frequency behavior is obtained:

$$F = \frac{\pi}{4\Delta^2}\omega[\min(\bar\mu, \Delta - \omega) - \max(-\Delta, \bar\mu - \omega)]. \tag{19}$$

This behavior is exhibited by the numerics, as shown in Fig. 2 (lower panel, see also discussion further below). Furthermore, in the low-frequency limit (19), we again recover the quadratic behavior described above on general grounds

$$F = \frac{\pi}{4\Delta^2}\omega^2. \tag{20}$$

Notice however that the proportionality constant is now independent of the filling factor. In Fig. 4, a more detailed comparison of the numerics with the analytical result of Eq.
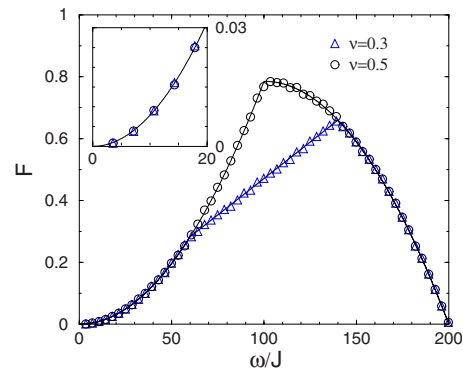

FIG. 4. (Color online) Comparison between numerics (symbols) and analytics [solid line, Eq. (19)] for *strong* disorder. The value of the disorder is $\Delta/J = 100$ and the filling factors are $\nu = 0.3$ and $\nu = 0.5$. The length of the chain is $M = 2000$ and the number of disorder realizations is $N_r = 2000$. In the inset, we compare our numerics with the quadratic expansion (20) expected at low frequency. In both cases, the agreement is quite good.
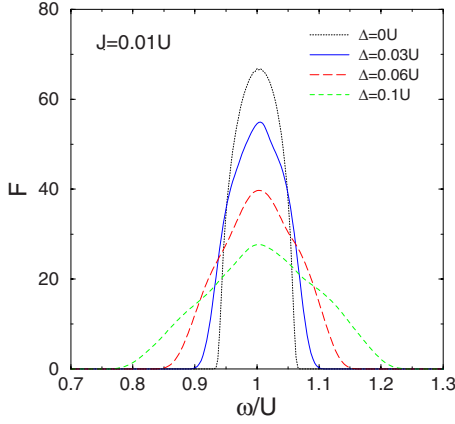
FIG. 5. (Color online) Energy absorption rate in the Mott insulator phase for hard-core bosons in a random potential: the response function F [see Eq. (14)] is plotted versus modulation frequency for fixed $J=0.01U$ and increasing values of the disorder strength $\Delta/U=0$ (black dotted line), $0.03, 0.06, 0.1$. The length of the chain is $M=60$ and the number of disorder realizations is $N_r=200$. A broadening of the absorption peak is observed for increasing disorder.

(19) for the limit of strong disorder is shown. In the inset, we also compare our numerical results with the quadratic behavior (20) expected at low frequency. In both cases, the agreement is remarkably good.

B. Unit filling

The absorption rate for $\nu=1$ is calculated numerically starting from Eqs. (11) and (12). The result is shown in Fig. 5 as a function of frequency for different values of the disorder strength Δ and $J=0.01U$.

In the absence of disorder ($\Delta=0$), the absorption rate can be evaluated analytically and the dimensionless function F in Eq. (14) is given by [23]

$$F = \frac{2\omega}{3J} \left| \sin\left[\cos^{-1}\left(\frac{\omega-U}{6J} \right) \right] \right|, \quad \text{for} |\omega-U| < 6J,$$

(21)

and vanishes otherwise. The dashed line in Fig. 5 corresponds to our numerical result for $\Delta=0$, which fully agrees with the above formula.

As the strength of disorder is increased, we see from Fig. 5 that the absorption spectrum becomes broader and progressively develops a trianglelike shape as the limit $J \ll \Delta$ is approached. This behavior can be obtained analytically starting from Eq. (13). In the $J \ll \Delta$ limit, since the on-site energies at different lattice sites are uncorrelated, we obtain

$$F \simeq \frac{\pi\omega}{2\Delta^2} \int_{-\Delta}^{\Delta} d\epsilon \int_{-\Delta}^{\Delta} d\epsilon' \, \delta(\omega-U+\epsilon-\epsilon'),$$

(22)

where $\bar{\rho}(\epsilon)=1/2\Delta$ is the disorder-averaged density of states in the atomic limit introduced above. Upon integration, Eq. (22) yields

$$F \simeq \frac{\pi\omega}{2\Delta^2}(2\Delta - |\omega-U|),$$

(23)

showing that the line shape of the absorption rate in the atomic limit is approximately triangular and vanishes at $|\omega - U| = 2\Delta$ for $J \ll \Delta$.

IV. QUASIPERIODIC POTENTIAL

In this section, we assume that the external potential in Eq. (1) is $\epsilon_j = \Delta \cos(2\pi j \sigma)$ [15–17], being σ an irrational number. This quasiperiodic potential distribution is realized experimentally by superimposing two different periodic potentials with incommensurate lattice periods [11]. Differently from the disorder potential considered in the previous section, where all states are localized (in the thermodynamic limit) for an arbitrarily small amount of disorder, in the quasiperiodic case there is a phase transition [32] at $\Delta_c=2J$: for $\Delta < 2J$ all states are *extended* while for $\Delta > 2J$ all states are *exponentially* localized.

As described below, we find that the absorption spectra of bosons in the quasiperiodic potential are remarkably different from the spectra described in Sec. III for the bosons moving on a disorder potential.

A. Incommensurate filling

For lattice fillings $\nu < 1$ (i.e., less than a boson per site), we calculate the absorption rate numerically starting from Eqs. (7) and (8). We restrict to zero temperature and fix $\sigma = 0.771\,452\,45$, which is relevant to the experiments carried out by the Florence group.

In Fig. 6 we plot the frequency dependence of the response function (14) for increasing values of the disorder strength Δ. Compared to Fig. 2, we see that the absorption spectra in quasiperiodic potential exhibit a much richer structure. Interestingly, the response function becomes very large (and actually diverges) when ω matches special values. Moreover, for a given filling factor, the absorption rate is nonzero only within a certain range of frequencies.

These features can again be understood in the limits of weak and at strong disorder, where results can be obtained analytically. In the limit $\Delta \ll J$, the absorption rate can be calculated starting from Eq. (9) and taking the thermodynamic limit. This yields ($\varepsilon_k = -2J \cos k$)

$$F = \frac{\pi\omega}{2} \int \frac{dk}{2\pi} \frac{dk'}{2\pi} \frac{|V(k-k')|^2}{J^2} \delta(\omega + \varepsilon_k - \varepsilon_{k'})$$
$$\times \Theta(\mu - \varepsilon_k)\Theta(\varepsilon_{k'} - \mu),$$

(24)

where the integration over momenta is restricted to $[0, 2\pi]$. Using that the (modulus square of the) Fourier transform of the disorder potential is $|V(k)|^2 = \lim_{M\to\infty} |V_M(k)|^2$, where

$$|V_M(k)|^2 = \frac{\Delta^2}{4M} \left| \frac{e^{i(k+k_0)M} - 1}{e^{i(k+k_0)} - 1} + \frac{e^{i(k-k_0)M} - 1}{e^{i(k-k_0)} - 1} \right|^2, \quad (25)$$

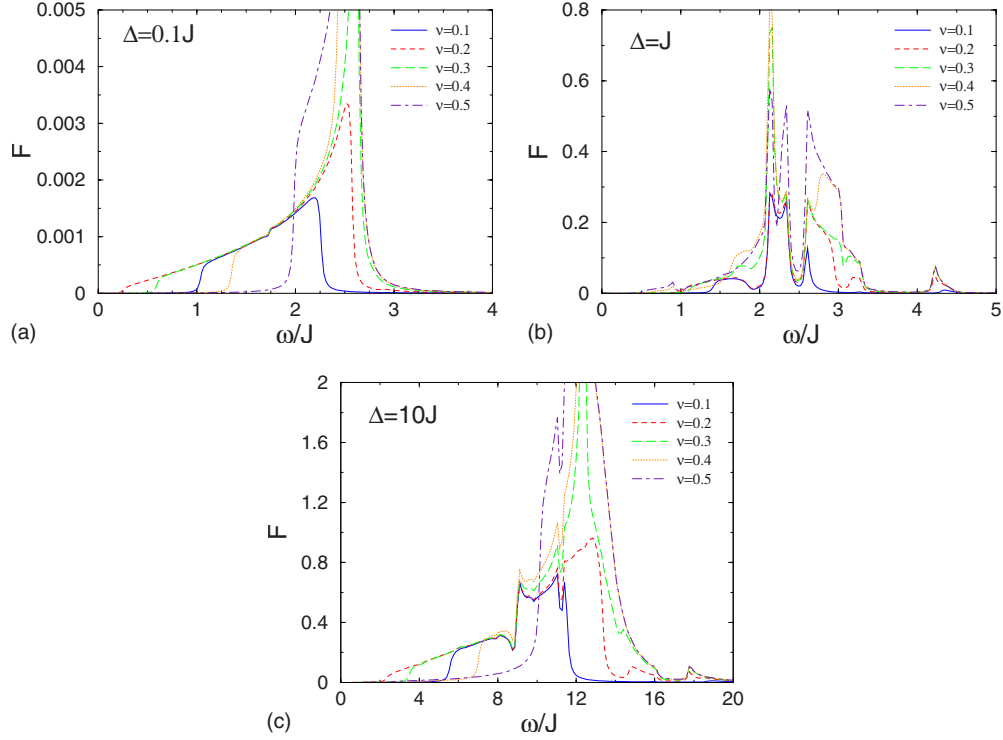and $k_0 = 2\pi\sigma$, for $M \to \infty$, the right-hand side of Eq. (25) becomes a series of delta functions

FIG. 6. (Color online) Energy absorption rate of hard-core bosons in a *quasiperiodic* potential with $\sigma=0.771\,452\,45$: the response function F [see Eq. (14)] is plotted versus modulation frequency for different filling factors and increasing values of disorder strength: $\Delta=0.1J$ (top panel), $\Delta=J$, and $\Delta=10J$. Calculations are done on a ring of $M=1200$ lattice sites yielding almost negligible finite-size effects. The number of disorder realization is $N_r=500$.

$$|V(k)|^2 = \frac{\pi\Delta^2}{2} \sum_{n=-\infty}^{+\infty} [\delta(k+k_0+2\pi n) + \delta(k-k_0+2\pi n)]. \quad (26)$$

Inserting Eq. (26) into Eq. (24), we obtain

$$F = \frac{\omega\pi\Delta^2}{4J^2} \int_0^{2\pi} \frac{dk}{2\pi} \delta(\omega+\varepsilon_k-\varepsilon_{k+k_0})$$
$$\times \Theta(\mu-\varepsilon_k)\Theta(\varepsilon_{k+k_0}-\mu). \quad (27)$$

The integral in Eq. (27) can be evaluated using the identity $a\sin k+b\cos k=c\cos(k+\gamma)$, where $c=\sqrt{a^2+b^2}$ and $\tan\gamma=-a/b$. Since $a=\sin k_0$ and $b=1-\cos k_0$, we obtain $c=2\sin(k_0/2)$ and $\tan\gamma=-1/\tan(k_0/2)$. The zeroes of the δ function in Eq. (27) occur at $k=k_\pm=-\gamma\pm\arccos(\omega/2Jc)$. Hence, we obtain

$$F = \frac{\Delta^2}{4J^2} \frac{\omega/2}{\sqrt{(2Jc)^2-\omega^2}} \sum_{r=\pm} \Theta(-\xi_r)\Theta(\omega+\xi_r), \quad (28)$$

where $\xi_r=\varepsilon_{k_r}-\mu=-2J\cos k_r-\mu$. Equation (28) shows that the absorption is finite only in a range of frequencies given by the conditions $\xi_r<0$ and $\xi_r+\omega>0$, where ξ_r itself depends on ω through the ω dependence of k_r. Moreover, the response diverges for $\omega=2Jc$, provided this frequency value is allowed for a given filling factor. Since $c=2\sin\pi\sigma=1.315\,76$, the divergence occurs at $\omega=2.631\,5J$, as found numerically and shown in Fig. 6 (upper panel).

For a potential strength comparable to the tunneling rate, i.e., $\Delta\sim J$, the absorption spectrum develops very sharp peaks as shown in the central panel of Fig. 6. These peaks gradually disappear as Δ increases and becomes much larger than J. In this regime, however, the energy absorption spectrum becomes indeed rather similar to the case of weak quasiperiodic potential, as can be seen by comparing the upper and lower panels of Fig. 6. This peculiar effect can be explained analytically starting from Eq. (10), which applies in the atomic limit. Introducing the variable $y=2\pi\sigma n$, in the thermodynamic limit, we obtain

$$F = \omega\pi \int_0^{2\pi} \frac{dy}{2\pi} \delta[\omega+\Delta\cos y-\Delta\cos(y+2\pi\sigma)]$$
$$\times \Theta(\mu-\Delta\cos y)\Theta(\omega+\Delta\cos y-\mu). \quad (29)$$

The integral in Eq. (29) becomes the integral in Eq. (27) after a change of variable $k=y+\pi$. We thus obtain

$$F = \frac{\omega/2}{\sqrt{(\Delta c)^2-\omega^2}} \sum_{r=\pm} \Theta(\mu+\Delta\cos k_r)\Theta(\omega-\Delta\cos k_r-\mu), \quad (30)$$

showing that the behavior of the absorption rate at strong quasiperiodic potential can be obtained from Eq. (28) by simply replacing $2J$ with Δ.

B. Unit filling

We have obtained the absorption spectrum at unit filling numerically using Eqs. (11) and (12), for the same value of
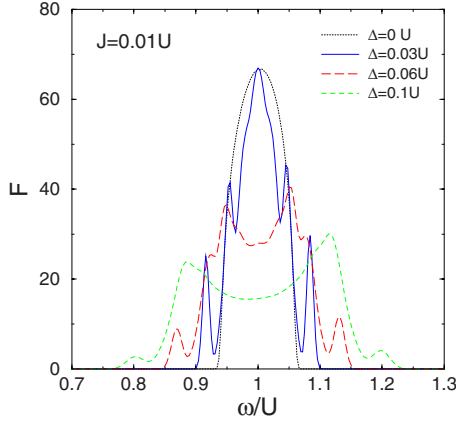
FIG. 7. (Color online) Energy absorption in the Mott insulator phase for bosons in a *quasiperiodic* potential with σ =0.771 452 45: the response function F [see Eq. (14)] is plotted versus modulation frequency for fixed $J=0.01U$ and increasing disorder strength $\Delta/U=0$(black dotted line), 0.03, 0.06, 0.1. Here, convergence is achieved for system size $L=70$. As disorder increases, the response function broadens and changes convexity, as predicted by Eq. (32).

$\sigma=0.771\ 452\ 45$. The result is plotted in Fig. 7 for fixed $J/U=0.01$ and increasing values of the quasiperiodic potential strength Δ. The dashed line corresponds to the clean case $\Delta=0$, where the absorption rate is given by Eq. (21).

We see that the shape of the absorption spectrum changes considerably as Δ increases. For sufficiently weak quasiperiodic potential $\Delta \lesssim 3\ J$, the spectrum does not become broad, but instead satellite peaks appear on the sides of the central absorption feature. For stronger quasiperiodic potentials, the central peak disappears and the spectrum develops a two hump structure. To understand these features, let us again focus on the atomic limit, where the absorption rate can be obtained analytically using Eq. (13). Introducing the variable $y=2\pi\sigma n$ and passing to the continuum limit, we obtain the result

$$F = 2\omega\pi \int_0^{2\pi} \frac{dy}{2\pi} \delta[\omega - U + \Delta\cos y - \Delta\cos(y+2\pi\sigma)].$$

(31)

The integral (31) can be readily evaluated using the identity $a\sin y+b\cos y=c\cos(y+\gamma)$, where $\tan\gamma=-a/b$ and $c=\sqrt{a^2+b^2}$. From Eq. (31) we have that $c=2\sin\pi\sigma$ and, therefore,

$$F = \frac{2\omega}{\sqrt{(\Delta c)^2 - (\omega - U)^2}},$$

(32)

showing that the absorption rate diverges at the edge, where $|\omega - U|=\Delta c$. This means that the shape of the absorption spectrum changes completely going from weak to strong quasiperiodic potential, as obtained numerically and shown in Fig. 7. Finally, in comparing Eqs. (23) and (32), we see that in a quasiperiodic potential the absorption spectrum is (at least in the atomic limit) narrower because $c<2$.
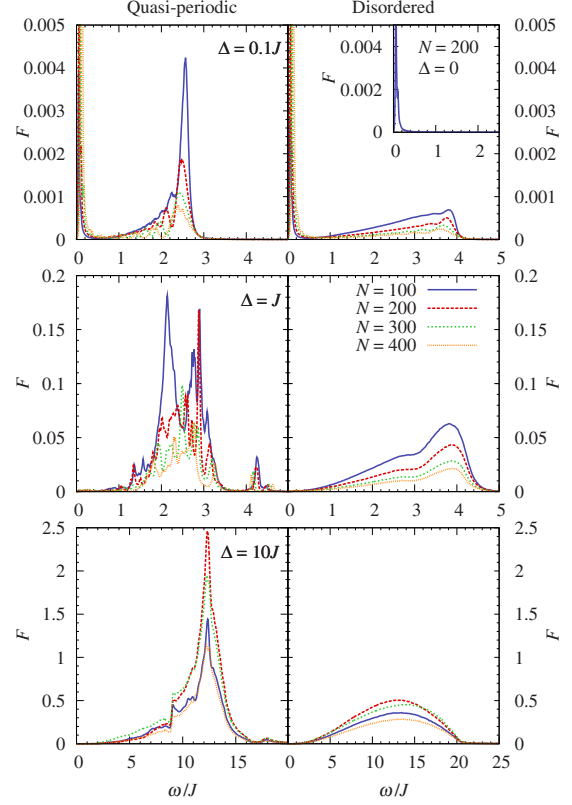

FIG. 8. (Color online) Energy absorption rate of disordered and quasidisordered hard-core bosons in a parabolic trap. The response function F is plotted versus modulation frequency for different fillings. Upper panel: $\Delta=0.1J$, middle panel: $\Delta=J$, and lower panel: $\Delta=10J$. The system size is $M=500$, the number of disorder realizations is $N_r=4000$, and $\alpha^{\rm ho}=2.88\times10^{-4}J$. The inset in the upper panel shows the low-frequency absorption in the absence of disorder, which is finite for trapped gases. As Δ increases, this sharp peak fragments out and is no longer visible on the scale of the bulk contribution.

V. EFFECTS OF A PARABOLIC TRAP

In this section, we discuss the effects of a harmonic trapping potential $V(z)=m\omega_{\rm ho}^2 z^2/2$ on the absorption spectrum. Here, m is the atom mass and $\omega_{\rm ho}$ is the trapping frequency. In this case, $V_j^{\rm ho}$ in Eq. (1) is nonzero and given by $V_j^{\rm ho}=\alpha^{\rm ho}(j-M/2)^2$, where $\alpha^{\rm ho}=m\omega_{\rm ho}^2 d^2/2$, d being the lattice period.

We have repeated the calculations of the absorption spectrum including $V_j^{\rm ho}$ and the result is shown in Fig. 8. For a system of hard-core bosons in the absence of disorder or quasiperiodic potential, the trap favors the formation of a Mott insulator in the center surrounded by a superfluid region at the trap edges. This gives rise to a finite absorption at low frequency (see inset in the upper panel), which is related to the creation of excitations at the edge of the trap. By contrast, in a uniform system of hard-core bosons, as we have described in Sec. II, the energy absorption vanishes to all orders because the hopping operator K commutes with the Hamiltonian.

Let us next consider the effect of a small amount of disorder or a weak quasiperiodic potential. Clearly, the Mott

insulator at the center of the trap cannot absorb energy at low frequency, so the only contribution comes from the outer shell, where the filling factor is less than unity. In particular, the low-frequency peak arising from edge excitations fragments in multiple peaks with little spectral weight compared to the response from the bulk discussed in Secs. III and IV.

We also see in Fig. 8 that the behavior of the absorption spectrum at frequencies close to the bandwidth crucially depends on whether the applied potential is truly random or quasiperiodic. Whereas the disordered case exhibits a smooth behavior in the absorption up to the bandwidth $4J$ where it falls to zero, the quasiperiodic one shows a sharp peak located at the bandwidth $4Jc$, which resembles the divergence found in the corresponding homogeneous case. Note that the position of this peak is almost independent on the number of atoms in the tube and, therefore, the peak should be visible in a realistic experimental situation, where an average over a multiple tube setup with variable filling is performed [33]. The same conclusion applies to the system with strong disorder or quasiperiodic potential as can be observed in the lower panel in Fig. 8. For $\Delta \sim J$ (Fig. 8, middle panel), the peak structure in the quasiperiodic case is more complex and, thus, the averaging procedure will produce some rounding off of the peaks. Still, the absorption can be considerably larger than in the disordered case and this difference should be clearly visible.

VI. CONCLUSIONS

In conclusion, we have investigated the energy absorbed by a disordered strongly interacting Bose gas in the presence of periodically modulated optical lattices. For filling factor less than one, the absorption rate has been calculated exactly in the hard-core limit via the Bose-Fermi mapping. For commensurate filling, corresponding to one boson per lattice site, the gas is a Mott insulator and can only absorb energy at much higher frequency (on the order of the repulsive interaction U). The disorder-induced broadening of the absorption spectrum has been calculated by restricting to the subspace of particle-hole excitations.

We have performed extensive calculations comparing two different sources of disorder: a random potential, which is relevant for current experiments based on speckle patterns, and a quasiperiodic potential, which is obtained by superimposing two optical lattices with incommensurate periods. Our results indicate that the response of the gas to the lattice modulation significantly depends on the chosen source of randomness.

APPENDIX

In this appendix, we shall derive the asymptotic formula (9) based on the perturbation theory for weak disorder. For clarity, we rewrite the general expression (7)

$$\dot{E}_\omega = \frac{\delta J_0^2 \pi \omega}{2} \sum_{k,k'} \mathcal{K}_{kk'}[f(\varepsilon_k) - f(\varepsilon_{k'})]\delta(\omega + \varepsilon_k - \varepsilon_{k'}),$$
(A1)

using new indices k and k'. Moreover, we find convenient to introduce the matrix elements

$$A_{kk'} = \sum_j [\psi_k^*(j+1)\psi_{k'}(j) + \psi_k^*(j)\psi_{k'}(j+1)], \quad \text{(A2)}$$

so that $\mathcal{K}_{k,k'} = |A_{k,k'}|^2$.

In the absence of disorder $\Delta = 0$, the eigenstates are plane waves $\psi_k^0(n) = e^{ikn}/\sqrt{L}$ with energy $\epsilon_k^0 = -2J \cos k$. Therefore, from Eq. (A2), we find

$$A_{kk'}^0 = 2\delta_{kk'} \cos k,$$
(A3)

showing that the matrix A is *diagonal* in momentum space. Since the matrix $\mathcal{K}_{kk'}^0 = 4\delta_{k,k'} \cos^2 k$ is also diagonal, the absorption rate (7) *vanishes*.

For $\Delta \ll J$, we formally expand the right-hand side of Eq. (A2) in powers of the disorder strength $A_{k,k'} = A_{kk'}^0 + A_{kk'}^1 + A_{kk'}^2 + O(\Delta^3)$, so the matrix $\mathcal{K}$ takes the form

$$\mathcal{K}_{k,k'} = \mathcal{K}_{kk'}^0 + A_{kk'}^0(A_{kk'}^1 + A_{k'k}^1 + A_{kk'}^2 + A_{k'k}^2) + |A_{kk'}^1|^2 + O(\Delta^3).$$
(A4)

Taking Eq. (A3) into account, we see that the only *nondiagonal* term appearing in the expansion (A4) is $|A_{kk'}^1|^2$, which is on the second order in Δ. This term can be readily evaluated from Eq. (A2) by applying the first-order perturbation theory for the eigenstates

$$\psi_k = \psi_k^0 + \sum_{q \neq k} \frac{\langle \psi_q^0 | V | \psi_k^0 \rangle}{\epsilon_k^0 - \epsilon_q^0} \psi_q^0.$$
(A5)

After a simple algebra, we obtain

$$A_{kk'}^1 = \frac{\langle \psi_k^0 | V | \psi_{k'}^0 \rangle}{\epsilon_k^0 - \epsilon_{k'}^0} 2(\cos k - \cos k'),$$
(A6)

which is valid up to the linear order in Δ. Finally, by using the dispersion relation $\varepsilon_k^0 = -2J \cos k$, Eq. (A6) further simplifies yielding

$$A_{kk'}^1 = \frac{\langle \psi_k^0 | V | \psi_{k'}^0 \rangle}{J}.$$
(A7)

Substituting Eq. (A6) into Eq. (A1) and replacing the eigenstates by their zero-order values $\epsilon_k = \epsilon_k^0$, we recover the asymptotic formula (9).

[1] I. Bloch, J. Dalibard, and W. Zwerger, Rev. Mod. Phys. **80**, 885 (2008).

[2] M. Greiner, O. Mandel, T. Esslinger, T. W. Hänsch, and I. Bloch, Nature (London) **415**, 39 (2002).

[3] A. F. Ho, M. A. Cazalilla, and T. Giamarchi, Phys. Rev. A **79**, 033620 (2009).

[4] J. E. Lye, L. Fallani, M. Modugno, D. S. Wiersma, C. Fort, and M. Inguscio, Phys. Rev. Lett. **95**, 070401 (2005).

[5] D. Clément, A. F. Varón, M. Hugbart, J. A. Retter, P. Bouyer, L. Sanchez-Palencia, D. M. Gangardt, G. V. Shlyapnikov, and A. Aspect, Phys. Rev. Lett. **95**, 170409 (2005).

[6] C. Fort, L. Fallani, V. Guarrera, J. E. Lye, M. Modugno, D. S. Wiersma, and M. Inguscio, Phys. Rev. Lett. **95**, 170410 (2005).

[7] T. Schulte, S. Drenkelforth, J. Kruse, W. Ertmer, J. Arlt, K. Sacha, J. Zakrzewski, and M. Lewenstein, Phys. Rev. Lett. **95**, 170411 (2005).

[8] Y. P. Chen, J. Hitchcock, D. Dries, M. Junker, C. Welford, and R. G. Hulet, Phys. Rev. A **77**, 033632 (2008).

[9] M. White, M. Pasienski, D. McKay, S. Q. Zhou, D. Ceperley, and B. DeMarco, Phys. Rev. Lett. **102**, 055301 (2009).

[10] U. Gavish and Y. Castin, Phys. Rev. Lett. **95**, 020401 (2005).

[11] L. Fallani, J. E. Lye, V. Guarrera, C. Fort, and M. Inguscio, Phys. Rev. Lett. **98**, 130404 (2007).

[12] J. Billy, V. Josse, Z. Zuo, A. Bernard, B. Hambrecht, P. Lugan, D. Clement, L. Sanchez-Palencia, P. Bouyer, and A. Aspect, Nature (London) **453**, 891 (2008).

[13] G. Roati, C. D'Errico, L. Fallani, M. Fattori, C. Fort, M. Zaccanti, G. Modugno, M. Modugno, and M. Inguscio, Nature (London) **453**, 895 (2008).

[14] G. Orso, Phys. Rev. Lett. **99**, 250402 (2007).

[15] G. Roux, T. Barthel, I. P. McCulloch, C. Kollath, U. Schollwöck, and T. Giamarchi, Phys. Rev. A **78**, 023628 (2008).

[16] X. Deng, R. Citro, A. Minguzzi, and E. Orignac, Phys. Rev. A **78**, 013625 (2008).

[17] T. Roscilde, Phys. Rev. A **77**, 063605 (2008).

[18] G. Roati, M. Zaccanti, C. D'Errico, J. Catani, M. Modugno, A. Simoni, M. Inguscio, and G. Modugno, Phys. Rev. Lett. **99**, 010403 (2007).

[19] T. Giamarchi and H. J. Schulz, Phys. Rev. B **37**, 325 (1988).

[20] M. P. A. Fisher, P. B. Weichman, G. Grinstein, and D. S. Fisher, Phys. Rev. B **40**, 546 (1989).

[21] D. Delande and J. Zakrzewski, Phys. Rev. Lett. **102**, 085301 (2009).

[22] T. Stöferle, H. Moritz, C. Schori, M. Köhl, and T. Esslinger, Phys. Rev. Lett. **92**, 130403 (2004).

[23] A. Iucci, M. A. Cazalilla, A. F. Ho, and T. Giamarchi, Phys. Rev. A **73**, 041608(R) (2006).

[24] C. Kollath, A. Iucci, T. Giamarchi, W. Hofstetter, and U. Schollwöck, Phys. Rev. Lett. **97**, 050402 (2006).

[25] C. Kollath, A. Iucci, I. P. McCulloch, and T. Giamarchi, Phys. Rev. A **74**, 041604(R) (2006).

[26] M. Hild, F. Schmitt, and R. Roth, J. Phys. B **39**, 4547 (2006).

[27] M. Hild, F. Schmitt, I. Türschmann, and R. Roth, Phys. Rev. A **76**, 053614 (2007).

[28] A. De Martino, M. Thorwart, R. Egger, and R. Graham, Phys. Rev. Lett. **94**, 060402 (2005).

[29] M. Albert, T. Paul, N. Pavloff, and P. Leboeuf, Phys. Rev. Lett. **100**, 250405 (2008).

[30] M. A. Cazalilla, Phys. Rev. A **70**, 041604(R) (2004).

[31] V. Golovach, A. Minguzzi, and L. Glazman, e-print arXiv:0907.0483.

[32] J. B. Sokoloff, Phys. Rep. **126**, 189 (1985).

[33] In current experiments, the lattice modulation technique requires a large modulation amplitude, which goes beyond the linear-response regime. These effects can be studied numerically using DMRG as done in Ref. [24] for the clean case. We leave that for future work.